# Polarization-Dependent Phase of Light Propagating in Optical Fibers

Luca Palmieri, *Senior Member, IEEE*, Martina Cappelletti, *Member, IEEE*, Marco Santagiustina, *Member, IEEE*, and Andrea Galtarossa, *Fellow, IEEE*

***Abstract*—As it propagates in a real single-mode fiber, light accumulates a phase delay and undergoes variations of its polarization state. These two phenomena are partly related to each other, owing to both well known geometric effects, i.e. the Pancharatnam's phase, and less known dynamic ones. This article aims at reviewing these concepts, highlighting the polarization-depended phase of light that propagates in a single-mode fiber. We present a mathematical treatment using the familiar language of Jones and Stokes vectors and report experiments supporting the theory. The presented analysis has a general validity, and it can describe phase variation with respect to several parameters, such as distance, frequency and time. Its extension to multimode and multi-core fibers is also discussed. The results can be used for a better modelling and understanding of coherent transmission systems and interferometric fiber optic sensors.**

***Index Terms*—Polarization, optical fibers, Pancharatnam phase, geometric phase, dynamic phase.**

## I. Introduction

IN 1956, S. Pancharatnam published a seminal paper proving that when the polarization of a light beam is changed over a cycle, also the phase of the light beam changes, and the amount of this phase change is related only to the trajectory that the polarization of the beam draws on the Poincaré sphere [1]. Pancharatnam's work, however, didn't received the due attention until the second half of the 1980 s, after M.V. Berry discovered the eponymous geometric phase in quantal systems [2] and Pancharatnam's phase was recognized as a special manifestation of it [3], [4]. Since then, there has been a flourishing research activity on geometric phase in photonic systems, including optical fibers [5], [6], [7].

It is worthwhile remarking, for completeness and clarity, that the scientific literature about geometric phase in optical fibers follows two distinct research lines: one focuses on the Pancharatnam's phase, the other (so far the most active one) focuses on the rotation of polarization of light propagated along a non-coplanar path, sometimes called Rytov-Vladimirskii-Berry phase [8]. Actually, soon after Berry's publication, some authors [9], [10] reported experiments showing how the polarization of light transmitted across a single-mode fiber, deployed along a helical path, undergoes a rotation that can be explained as a manifestation of Berry's geometric phase. Berry himself argued that the phenomenon is better described in terms of parallel transport of light polarization [11], as previously observed by Ross [12] and subsequently by other authors [6], [13], [14], [15], [16], [17], [18], [19]. Parallel transport of light is a manifestation of classical anholonomy, and it has been originally studied in the framework of ray optics [20]. Despite it shares a similar theoretical framework with the Pancharatnam's phase, parallel transport of polarization is a distinct phenomenon, and we do not considered it in this article.

Pancharatnam's phase is related to variations of the light polarization and it can accumulate also when light propagates along straight or planar paths. While physically different from the Rytov-Vladimirskii-Berry phase, also Pancharatnam's phase can be interpreted as a parallel transport, but in this case occurring on the Poincaré sphere. Only a few papers have analyzed this phenomenon in optical fibers, in the framework of both telecommunications [21], [22] and sensing [23], [24], [25]. Nonetheless, to the best of our knowledge a general theoretical model unifying polarization effects in randomly birefringent single-mode fibers and the Pancharatnam's phase has never been reported. Following the guidelines of theoretical analyses made about Berry's phase in quantum systems, in this article we highlight how the phase of the light field can be decomposed in two terms: one is independent of polarization, while the other is dependent on polarization; we call this term "polarization-dependent phase" (PDP). As we show later, PDP is given by two terms: one is the Pancharatnam's phase, the other is a dynamical phase related to birefringence.

We remark that this is only a decomposition of the total phase and, sure enough, any modelling or measurement based on Jones formalism already implicitly includes the PDP. Nevertheless, we believe that singling it out can contribute to a better modelling and understanding of fiber-based coherent transmission systems and interferometric sensors.

The article is organized as follows. Section II presents the theoretical framework and the main result of this article, namely

Manuscript received 24 February 2023; revised 19 June 2023; accepted 3 July 2023. Date of publication 10 July 2023; date of current version 2 November 2023. This work was supported in part by European Union through the Italian National Recovery and Resilience Plan NRRP of Next Generation EU, partnership on "Telecommunications of the Future" (PE0000001 - program "RESTART") and in part by MIUR (PRIN 2017, Project FIRST). *(Corresponding author: Luca Palmieri.)*

The authors are with the Department of Information Engineering, University of Padova, 35131 Padova, Italy, and also with the CNIT, National Inter-University Consortium for Telecommunications, 43124 Parma, Italy (e-mail: luca.palmieri@unipd.it; martina.cappelletti.1@phd.unipd.it; marco.santagiustina@unipd.it; andrea.galtarossa@unipd.it).

Color versions of one or more figures in this article are available at https://doi.org/10.1109/JLT.2023.3293638.

Digital Object Identifier 10.1109/JLT.2023.3293638

(12); an example of application to the simple scenario of birefringence waveplates is also discussed. Section III reports experimental results supporting the theoretical analysis. Finally, Section IV discusses the extension of the model to multimode and multicore fibers. In the following, we explicitly refer to optical fibers, yet the results do apply to any other waveguide. For the sake of readability, mathematical derivations and technical details are deferred to the Appendices.

## II. Theoretical Analysis

Before presenting the polarization-dependent phase, we deem worthwhile recalling the key aspects of Pancharatnam's analysis. Given two scalar waves at the same frequency, it is rather natural to say whether these are in phase or not. Pancharatnam was the first to address the same problem for vector waves, proposing a natural, yet powerful, extension of the scalar concept [1], [4], [26]. Let $\boldsymbol{a}_0$ be the Jones vector of a reference wave and let $\boldsymbol{a}$ be that of an arbitrary wave; according to Pancharatnam, the two waves are said to be in phase when the intensity of their interference is maximum. Mathematically, this intensity reads

$$|\boldsymbol{a}_0+\boldsymbol{a}|^2=|\boldsymbol{a}_0|^2+|\boldsymbol{a}|^2+2\,|\boldsymbol{a}_0^*\boldsymbol{a}|\cos\big(\arg(\boldsymbol{a}_0^*\boldsymbol{a})\big)\,, \tag{1}$$

so the two waves are in phase when the argument of $\boldsymbol{a}_0^*\boldsymbol{a}$ is zero (hereinafter $^*$ represents transposition and conjugation). Equation (1) defines the so called "Pancharatnam's connection", and it allows to define the phase of $\boldsymbol{a}$ with respect to $\boldsymbol{a}_0$ as

$$\psi=\arg(\boldsymbol{a}_0^*\boldsymbol{a})\,. \tag{2}$$

Note, however, that in general this phase is *not* the Pancharatnam's phase, as clarified later.

Pancharatnam's connection has two important properties. The first one is that it is invariant with respect to changes of the state of polarization (SOP) of $\boldsymbol{a}$ that are represented on the Poincaré sphere by the geodesic (great circle) passing though the points $\hat{s}_0$ and $\hat{s}$ — i.e. the unit Stokes vectors associated to $\boldsymbol{a}_0$ and $\boldsymbol{a}$, respectively [27]. The second property is that the Pancharatnam's connection is *not transitive* [26], which means that if $\boldsymbol{a}$ is in phase with $\boldsymbol{a}_0$ and also another wave $\boldsymbol{a}'$ is in phase with $\boldsymbol{a}_0$, there is no guarantee that $\boldsymbol{a}$ and $\boldsymbol{a}'$ are in phase. This non-transitivity has an important consequence. Assume that $\boldsymbol{a}$ has the same polarization of $\boldsymbol{a}_0$, so they are represented by the same point $\hat{s}_0$ on the Poincaré sphere. Assume now that the polarization of the wave $\boldsymbol{a}$ is varied along a closed trajectory on the Poincaré sphere; then, it can be proved that the final phase of $\boldsymbol{a}$ with respect to $\boldsymbol{a}_0$ is varied by a quantity equal to $-1/2$ times the area encircled by the closed trajectory [4]. This phase is purely geometric and it is called *Pancharatnam's phase*. These properties of Pancharatnam's connection have been analyzed in several papers [26]; for the sake of completeness, we review them also in Appendix A.

Note that, in general, the Pancharatnam's phase is just one contribution to $\psi$. Actually, we highlight in the following that the phase difference between the two waves $\boldsymbol{a}$ and $\boldsymbol{a}_0$ can be decomposed in the sum of three terms:

$$\psi=\arg(\boldsymbol{a}_0^*\boldsymbol{a})=\sigma+\chi+\gamma\,. \tag{3}$$

The first one, $\sigma$, is the *dynamic scalar phase*; it is said "dynamic" because it depends on the effective refractive index seen by the propagating light (i.e. on its propagation velocity) and "scalar" because it is independent of polarization. The second term, $\chi$, is the *dynamic polarization-dependent phase*; it depends on fiber birefringence (hence it is still a "dynamic" term) and on light polarization. To understand this term, we can think about a polarization maintaining fiber: depending on whether the input SOP is aligned with the fast or slow axis, the actual phase delay is smaller or larger; as we will see, $\chi$ capture this fact and generalizes it to arbitrary polarization. Finally, $\gamma$ is the geometric Pancharatnam's phase introduced before; it is said "geometric" because it depends only on how the polarization of light varies. In the next section we derive the expressions of these terms.

### A. Calculation of the PDP

To evaluate $\psi$, it is better to analyze how it varies with respect to a parameter. From a mathematical point of view, which parameter we choose is immaterial; however, just for reference, we consider the distance of propagation, $z$. Therefore, we now focus on $\psi(z)=\arg[\boldsymbol{a}_0^*\boldsymbol{a}(z)]$, which is the phase of the propagating wave $\boldsymbol{a}(z)$ with respect to the fixed reference $\boldsymbol{a}_0$. In general we can write [27], [28]

$$\partial\boldsymbol{a}(z)=-j\boldsymbol{K}(z)\boldsymbol{a}(z)\,, \tag{4}$$

where $\partial$ indicates derivative with respect to $z$,

$$\boldsymbol{K}(z)=\kappa_0(z)\boldsymbol{\Lambda}_0+\bar{\kappa}(z)\cdot\bar{\boldsymbol{\Lambda}}\,, \tag{5}$$

$\boldsymbol{\Lambda}_0$ is the identity matrix, $\bar{\boldsymbol{\Lambda}}$ is the vector of Pauli matrices, $\kappa_0=\beta_0-j\alpha_0$ ($\beta_0$ is the propagation constant, $\alpha_0$ the attenuation coefficient), and $\bar{\kappa}=(\bar{\beta}-j\bar{\alpha})/2$, with $\bar{\beta}(z)$ the birefringence vector and $\bar{\alpha}(z)$ the local dichroism vector, both of which are real and three-dimensional [27], [28]. Following the analysis performed in Ref. [29] for quantum systems, we introduce the transformed wave $\boldsymbol{b}(z)$ as (see Appendix B-A)

$$\boldsymbol{b}(z)=\exp\left\{j\int_0^z\xi(z')dz'\right\}\boldsymbol{a}(z)\,, \tag{6}$$

where

$$\xi=\frac{\mathrm{Re}\,[\boldsymbol{a}^*\boldsymbol{K}\boldsymbol{a}]}{\boldsymbol{a}^*\boldsymbol{a}}=\mathrm{Re}\,[\kappa_0+\bar{\kappa}\cdot\hat{s}]=\beta_0+\frac{1}{2}\bar{\beta}\cdot\hat{s}\,, \tag{7}$$

and $\hat{s}(z)=\boldsymbol{a}^*(z)\bar{\boldsymbol{\Lambda}}\boldsymbol{a}(z)$ is the unit Stokes vector associated to $\boldsymbol{a}(z)$ and $\boldsymbol{b}(z)$ [27], [28]. Note that $\xi$ does not depend on the local dichroism. Using (6) we have

$$\psi(z)=\arg[\boldsymbol{a}_0^*\boldsymbol{a}(z)]=-\int_0^z\xi(z')dz'+\arg[\boldsymbol{a}_0^*\boldsymbol{b}(z)]\,; \tag{8}$$

we will see that the first term is equal to $\sigma+\chi$ and accounts only for the dynamic phases (both scalar and polarization-dependent), while the second term is the Pancharatnam's phase, $\gamma$.

We now proceed to derive a differential equation for the phase $\gamma(z)$ of the Pancharatnam's connection $p(z)=\boldsymbol{a}_0^*\boldsymbol{b}(z)$. Note that $\boldsymbol{b}(z)$ obeys the equation

$$\partial\boldsymbol{b}=-j(\boldsymbol{K}-\xi\boldsymbol{\Lambda}_0)\boldsymbol{b}=-j\boldsymbol{H}\boldsymbol{b} \tag{9}$$

therefore, $\partial p=-j\boldsymbol{a}_0^*\boldsymbol{H}\boldsymbol{b}$. Moreover, $e^{j\gamma}=p/|p|$ and hence

$$\partial\gamma=j(p\,\partial p^*-p^*\partial p)/(2\,|p|^2)\,, \tag{10}$$

which leads to the final expression (see Appendix B-A)

$$\partial\gamma=-\frac{(\hat{s}_0\times\hat{s})\cdot\partial\hat{s}}{2(1+\hat{s}_0\cdot\hat{s})}\,, \tag{11}$$

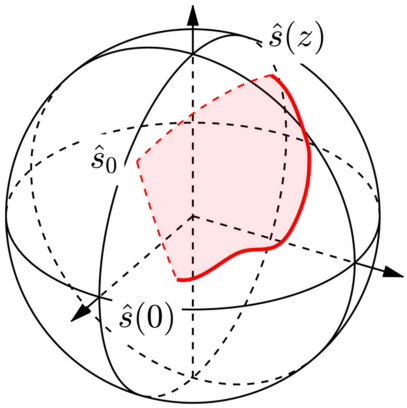


Fig. 1. The Pancharatnam's phase $\gamma(z)$ given by (16) is equal to $-1/2$ the solid angle subtended by the shaded area. Solid curve: trajectory of the SOP; dashed curves: geodesics connecting the reference SOP $\hat{s}_0$ and the edges of the SOP trajectory.

where $\hat{s}_0$ is the unit Stokes vector associated to the reference wave $\boldsymbol{a}_0$. Summarizing, we have found that the variation per unit length of the phase $\psi(z) = \arg[\boldsymbol{a}_0^* \boldsymbol{a}(z)]$ is

$$\partial\psi = -\beta_0 - \frac{1}{2}\bar{\beta}\cdot\hat{s} - \frac{(\hat{s}_0 \times \hat{s})\cdot\partial\hat{s}}{2(1+\hat{s}_0\cdot\hat{s})}, \tag{12}$$

which is the main theoretical results of this paper.

We recognize that

$$\sigma(z) = -\int_0^z \beta_0(z')dz' \tag{13}$$

is the dynamic scalar phase; it does not depend on light polarization but only on the effective refractive index of the mode propagating in the fiber. The second term yields the dynamic polarization-dependent phase

$$\chi(z) = -\frac{1}{2}\int_0^z \bar{\beta}(z')\cdot\hat{s}(z')dz'. \tag{14}$$

Recalling the example of the polarization maintaining fiber for which $\bar{\beta}$ is constant and eigenstates of polarization exist, we see that when the SOP is parallel or antiparallel to $\bar{\beta}$, the quantity $\sigma + \chi$ correctly represents the scalar phase delay associated to the propagation along the fast and slow axes of birefringence. Equation (14) generalizes this concept for arbitrary birefringence vectors and arbitrary SOPs. Note that it does not depend explicitly on the local dichroism vector $\bar{\alpha}$; yet, it depends implicitly on $\bar{\alpha}$ through the variation of $\hat{s}$ as a function of $z$.

Finally, the third term leads to the Pancharatnam's phase

$$\gamma(z) = -\frac{1}{2}\int_0^z \frac{[\hat{s}_0 \times \hat{s}(z')]\cdot\partial\hat{s}(z')}{1+\hat{s}_0\cdot\hat{s}(z')}dz', \tag{15}$$

which can be rearranged as (see Appendix B-B)

$$\gamma(z) = -\frac{1}{2}\int_{\mathcal{C}(z)} \frac{[\hat{s}_0 \times \hat{s}]\cdot\partial\hat{s}}{1+\hat{s}_0\cdot\hat{s}}, \tag{16}$$

where $\mathcal{C}(z)$ is the trajectory that, on the Poincaré sphere, goes from $\hat{s}_0$ to $\hat{s}(0)$ along the shortest geodesic, then follows the trajectory of the SOP up to $\hat{s}(z)$, and finally goes back to $\hat{s}_0$ again along the shortest geodesic (see Fig. 1). This quantity is purely geometric in the sense that it depends only on the trajectory $\mathcal{C}(z)$ and, as known, it is equal to $-1/2$ times the area encircled by the path $\mathcal{C}(z)$ (see Appendix B-B). The sign of this area is taken to be positive when the path is traversed in counterclockwise direction, negative otherwise. Notice that $\gamma$ is implicitly dependent on both $\bar{\beta}$ and $\bar{\alpha}$.

We define the polarization-dependent phase $\psi_{\text{pol}}(z)$ as the sum of the last two phase terms:

$$\psi_{\text{pol}}(z) = \chi(z) + \gamma(z). \tag{17}$$

The PDP is the only phase term that depends on (and only on) the polarization-related aspects of wave propagation, while being independent of the scalar ones. On the contrary, the dynamic scalar phase $\sigma$ is the only phase term independent of polarization aspect. As an example, a temperature variation occurring along a fiber do have an impact on $\sigma$, whereas it does not affect the PDP, as long as it is not changing the fiber birefringence (or dichroism). On the contrary, if for instance the SOP launched into a fiber is changed, we might expect the output phase to vary because of the PDP term, while $\sigma$ will remain unchanged.

Examples of application of this decomposition to simple optical elements as birefringent waveplates and polarizers are discussed for completeness in Appendix C.

### B. PDP With Respect to a Varying Reference Wave

In the previous sections we have focused the attention to the case in which the reference wave $\boldsymbol{a}_0$ is fixed. Considering for example a coherent receiver (either homodyne or heterodyne) this is indeed a common case. Nevertheless, there is an interest in analyzing also how the phase of the field $\boldsymbol{a}_2(z)$ varies with respect to another non-fixed field $\boldsymbol{a}_1(z)$, which is a function of $z$ too (we recall that the choice of the parameter $z$ is arbitrary). Basically, we are interested in the phase of the product $p_{2,1}(z) = \boldsymbol{a}_1(z)^* \boldsymbol{a}_2(z)$.

As examples of application of this problem, we may consider two fields $\boldsymbol{a}_1(z)$ and $\boldsymbol{a}_2(z)$ propagating along the same fiber, but launched with different input SOPs and/or with different frequencies (so to experience different birefringence). Another case that falls within this model is suggested in the recent analysis reported in Ref. [25]. In that paper, the authors used a phase-sensitive OTDR to measure, as a function of time, the phase of the light backscattered from a point beyond a polarization scrambler with respect to the phase of the light backscattered from a point before it. Strictly speaking, this is still the case in which the reference wave is constant (in this case with respect to time); nevertheless, if that kind of measurement have to be put in practice, it is likely that the SOP will vary over time at different points along the fiber, so that also the reference wave cannot be considered fixed.

At a first glance one may (erroneously!) think that the phase of $p_{2,1}(z)$ is equal to the difference between the phases of $\boldsymbol{a}_2(z)$ and $\boldsymbol{a}_1(z)$ evaluated with respect to a common fixed field $\boldsymbol{a}_0$. Actually, the fact that the Pancharatnam's connection is not transitive makes the above solution wrong, and the correct solution less trivial.

Following the guidelines of Section II-A, we highlight the dynamic phase term of both fields by factorizing them according

to (6):

$$\boldsymbol{a}_n(z) = \exp\left\{-j\int_0^z \xi_n(z')dz'\right\}\boldsymbol{b}_n(z)\,, \tag{18}$$

where $\xi_n = \beta_{0,n} + \bar{\beta}_n \cdot \hat{s}/2$ and $n = 1,\ 2$. It is then straightforward to express the phase difference as

$$\begin{aligned}\psi_{2,1}(z) &= \arg(p_{2,1}(z)) \\ &= \int_0^z \xi_1(z')dz' - \int_0^z \xi_2(z')dz' + \arg[\boldsymbol{b}_1^*(z)\boldsymbol{b}_2(z)]\,;\end{aligned} \tag{19}$$

this indicates that for what concerns the dynamic phases, the contribution to $\arg(p_{2,1}(z))$ is indeed simply the difference between the dynamic phases of each field (i.e. the first two integrals); differently, the geometric phase is given by the argument of $\boldsymbol{b}_1^*\boldsymbol{b}_2$. Proceeding in a way similar to what done in Section II-A, we find that the derivative of the phase $\gamma_{2,1}(z) = \arg[\boldsymbol{b}_1^*(z)\boldsymbol{b}_2(z)]$ reads

$$\partial\gamma_{2,1} = -\frac{1}{2}\left\{\frac{(\hat{s}_1\times\hat{s}_2)\cdot\partial\hat{s}_2}{1+\hat{s}_1\cdot\hat{s}_2} - \frac{(\hat{s}_1\times\hat{s}_2)\cdot\partial\hat{s}_1}{1+\hat{s}_1\cdot\hat{s}_2}\right\}. \tag{20}$$

Mathematically, both terms of this expression are similar to the analogous term of (11); yet, the crucial difference is that in (20) all the vectors depend on $z$, whereas in (11) $\hat{s}_0$ is independent of $z$.

The geometrical interpretation of (20) is less straightforward. Nevertheless, resorting to the arguments presented in Ref. [4], we can conclude that

$$\begin{aligned}\gamma_{2,1}(z) = &-\frac{1}{2}\int_0^z \frac{(\hat{s}_1\times\hat{s}_2)\cdot\partial\hat{s}_2}{1+\hat{s}_1\cdot\hat{s}_2}dz' \\ &+\frac{1}{2}\int_0^z \frac{(\hat{s}_1\times\hat{s}_2)\cdot\partial\hat{s}_1}{1+\hat{s}_1\cdot\hat{s}_2}dz'\,.\end{aligned} \tag{21}$$

is equal to the area encircled by the closed path that goes from $\hat{s}_1(0)$ to $\hat{s}_2(0)$ along the shortest geodesic arc, then follows the trajectory of $\hat{s}_2$ up to $\hat{s}_2(z)$, goes to $\hat{s}_1(z)$ along the shortest geodesic arc, and finally back to $\hat{s}_1(0)$ following the trajectory of $\hat{s}_1$.

In conclusion, the phase of $\boldsymbol{a}_2(z)$ with respect to $\boldsymbol{a}_1(z)$ is equal to the difference between the dynamic phases of $\boldsymbol{a}_2$ and those of $\boldsymbol{a}_1$ (both the scalar and polarization-dependent terms), plus the geometric contribution given by (21).

## III. Experimental Analysis

Since measuring phase and polarization of light as a function of the distance of propagation is not viable, to verify the above theory we setup an experiment to measure phase and polarization of the light transmitted across a fiber link as a function of the angular frequency $\omega$. The idea is to measure the complex wave $\boldsymbol{a}(\omega)$, for $\omega$ varying in a given range, and to analyze its phase with respect to a reference frequency $\omega_0$; in fact, we want to measure and analyze the phase

$$\psi(\omega) = \arg\big(\boldsymbol{a}^*(\omega_0)\boldsymbol{a}(\omega)\big)\,. \tag{22}$$

In this context, the dynamic polarization-dependent phase $\chi$ given by (14) is

$$\chi(\omega) = -\frac{1}{2}\int_{\omega_0}^{\omega} \bar{\Omega}(\omega')\cdot\hat{s}(\omega')d\omega'\,, \tag{23}$$

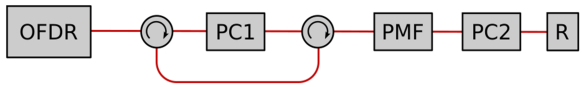


Fig. 2. Schematic of the experimental setup. OFDR, optical frequency domain reflectometer; PC, polarization controller; PMF, polarization maintaining fiber; R, reflector.

where $\bar{\Omega}$ is the polarization mode dispersion (PMD) vector of the fiber link. Similarly, according to (16), the Panchratnam phase is given by

$$\gamma(\omega) = -\frac{1}{2}\int_{\mathcal{C}(\omega)} \frac{[\hat{s}_0\times\hat{s}]\cdot\partial\hat{s}}{1+\hat{s}_0\cdot\hat{s}}\,, \tag{24}$$

where the only differences are that $\hat{s}_0 = \hat{s}(\omega_0)$ and the path $\mathcal{C}(\omega)$ is now a function of frequency.

Fig. 2 shows the experimental setup, which is built around a commercial optical frequency domain reflectometer (OFDR; Luna OBR 4600). The use of a commercial OFDR simplifies the experiment, because the device guarantees the linearity of the frequency sweep, includes a polarization diversity receiver that measures $\boldsymbol{a}(\omega)$, and enables performing the measurements on a relatively short time scale of about two seconds. The OFDR is connected to an optical circuit made of two circulators and one polarization controller (PC1), which is needed to change the SOP of the light launched into the fiber, without affecting that of the backscattered light. This control of the input SOP is necessary to calculate the PMD vector of the fiber link [30]. In order to have nontrivial polarization effects, the fiber link should have non-negligible polarization mode dispersion (PMD). For this reason, the link is made of a polarization maintaining fiber (PMF; $5\,\mathrm{m}$ long for about $6.2\,\mathrm{ps}$ of differential group delay), followed by a second polarization controller (PC2) and a reflector (R). This reflector (basically, a fiber-coupled mirror) makes Rayleigh scattering from the fiber negligible. Moreover, the polarization controllers are made with Lefevre's loops [31], and as a consequence, the total PMD of link includes the effects of the two circulators (estimated in the order of $0.1\,\mathrm{ps}$ to $0.2\,\mathrm{ps}$ per passage) and of the double passage along the PMF, making the frequency dependence of the total PMD vector nontrivial.

Five different input SOPs have been launched in the fiber link and the corresponding reflected complex light waves $\boldsymbol{a}(\omega)$ have been measured over $4.5\,\mathrm{THz}$ around $1550\,\mathrm{nm}$. The frequency was scanned at about $20\,\mathrm{nm/s}$, so the measurements lasted about $1.8\,\mathrm{s}$ each. Using these measurements, the transmitted SOPs and the PMD vector $\bar{\Omega}(\omega)$ of the link have been calculated according to the method described in Ref. [30].

The upper graph of Fig. 3 shows the measured differential group delay (DGD), $\Delta\tau = |\bar{\Omega}|$, whereas Fig. 4(a) shows the vector $\bar{\Omega}/\Delta\tau$ (i.e. the principal state of polarization [27]) drawn on the Poincaré sphere. Similarly, the lower graph of Fig. 3 shows, as an example, the second component of the transmitted SOP for the first input SOP; the corresponding complete SOP trajectory $\hat{s}(\omega)$ is shown in Fig. 4(b) as a function of frequency. Using these data, the different terms of the PDP have been calculated, adopting as reference the field transmitted at the

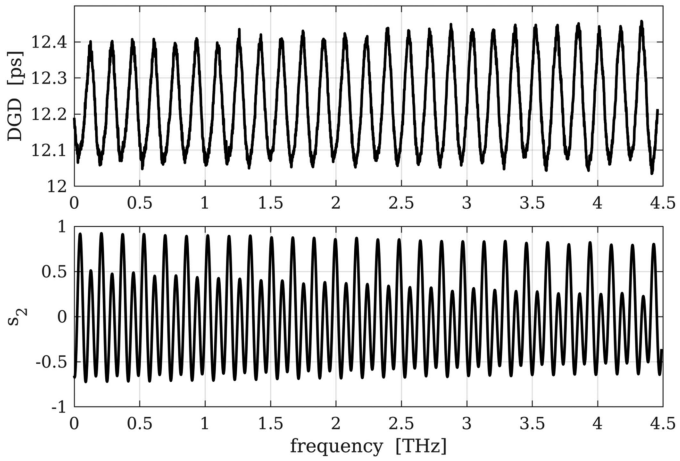


Fig. 3. DGD of the fiber link (upper graph) and second component of the transmitted SOP (lower graph) measured as a function of frequency.

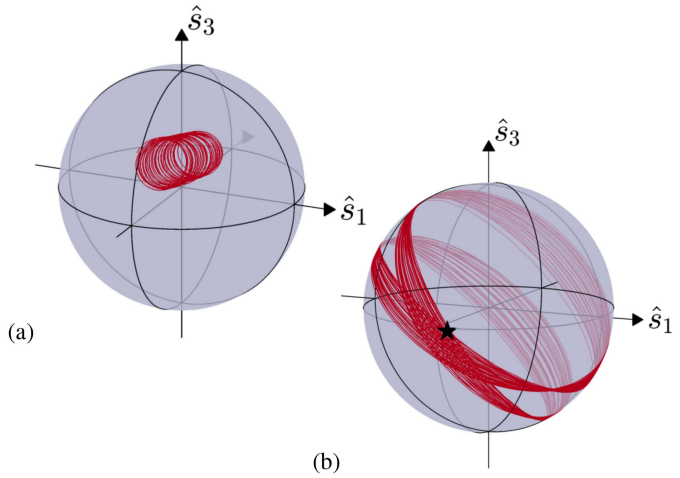


Fig. 4. Trajectory on the Poincaré sphere as a function of frequency of (a) the principal state of polarization of the fiber link and (b) one of the transmitted SOP (the $\hat{s}_2$ axis is pointing beyond the spheres in both cases). The black star indicate the SOP of the field used as a reference for the calculation of the phase terms.

lowest frequency, whose SOP is indicated by the star in Fig. 4(b). The blue curve in Fig. 5(a) represents the phase $\psi(\omega)$ calculated according to (22). The quantity is characterized by marked oscillations with the same period as the DGD, suggesting that they are due to polarization effects. In the same figure, the red curve represents the Pancharatnam's phase $\gamma(\omega)$ calculated according to (24); again the quantity shows similar marked oscillations. Finally, the green curve is the dynamic polarization-dependent phase $\chi(\omega)$, calculated using (23); while here the oscillations are less marked, they still have the same period. According to (3), the dynamic scalar phase is $\sigma = \psi - \chi - \gamma$, and it is shown in Fig. 5(a) by the black curve. In practice, $\sigma(\omega)$ represents the scalar phase effect due to the environmental perturbations acting on the fiber circuit during the measurement, which we recall lasted about $1.8\,\mathrm{s}$. It is remarkable that, some residual oscillations apart likely due to environmental noise, $\sigma$ does not show oscillations evidently related to polarization effects, confirming its scalar nature.

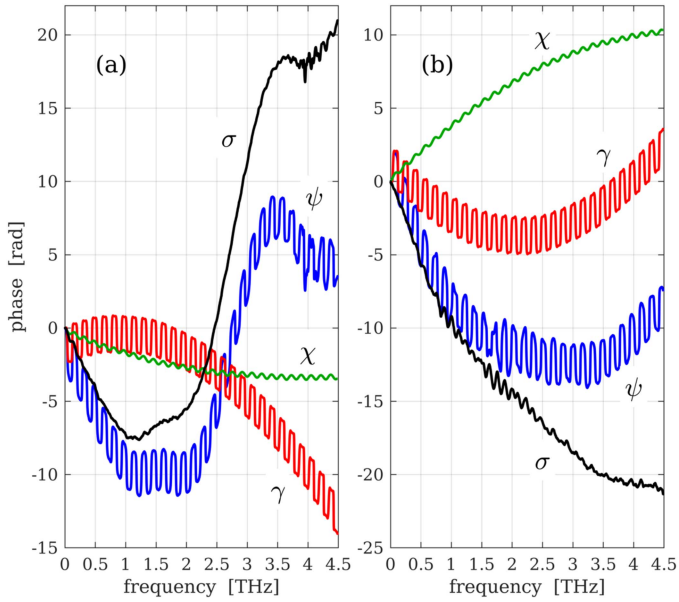


Fig. 5. Phases measured for two different input SOP, (a) and (b), respectively, plotted as a function of the frequency $\omega/(2\pi)$. For both graphs, curves represent the phase $\psi = \arg(\boldsymbol{a}^*(\omega_0)\boldsymbol{a}(\omega))$, the Pancharatnam's phase $\gamma$, the dynamic polarization-dependent phase $\chi$, and the dynamic scalar phase $\sigma$, as indicated on the graphs. Graphs share the same units on the vertical axes.

Fig. 5(b) shows a similar analysis performed on another input SOP. As we see, the above remarks and conclusions are confirmed, supporting the proposed decomposition of the phase $\psi$ in terms of polarization-dependent and polarization-independent terms.

## IV. Multimode and Multicore Fibers

The above analysis can be extended to multimode propagation, including the case of multicore fibers, although there is no simple geometrical interpretation.

The propagation of $M$ modes (counting both spatial and polarization modes) can be described by the $M$-dimensional generalized Jones vector $\boldsymbol{a}$ (also called state vector by some authors [28]), which represents amplitude and phase of the modes. It is useful to introduce the coherence matrix associated to $\boldsymbol{a}$, defined as $\boldsymbol{\mathcal{A}} = \boldsymbol{a}\boldsymbol{a}^*$. The propagation of the modes along the fiber is still described by (4), where $\boldsymbol{K}(z)$ is now the $M \times M$ complex coupling matrix (as before, we consider without loss of generality the dependence of $\boldsymbol{a}$ on $z$; yet the following analysis holds also for any other dependence). Similarly, also the transformed vector $\boldsymbol{b}(z)$ defined by (6) can be generalized to the $M$-dimensional case in a straightforward way, with $\xi$ expressed as

$$\xi = \frac{\mathrm{Re}\,[\boldsymbol{a}^*\boldsymbol{K}\boldsymbol{a}]}{\boldsymbol{a}^*\boldsymbol{a}} = \frac{\mathrm{Re}\,[\mathrm{tr}(\boldsymbol{K}\boldsymbol{\mathcal{A}})]}{\mathrm{tr}(\boldsymbol{\mathcal{A}})}\,, \tag{25}$$

where $\mathrm{tr}(\boldsymbol{X})$ is the trace of a matrix $\boldsymbol{X}$. As discussed in Refs. [29] and [32], $\xi$ is the dynamic phase variation per unit length of the wave $\boldsymbol{a}$. Similarly to the single-mode case, it can be decomposed in a scalar term and in a mode-dependent term.

Actually, the coherence matrix $\boldsymbol{\mathcal{A}}$ can be decomposed as

$$\boldsymbol{\mathcal{A}} = \frac{1}{M}(A_0\boldsymbol{\Lambda}_0 + \bar{A}\cdot\bar{\boldsymbol{\Lambda}})\,, \tag{26}$$

where now $\boldsymbol{\Lambda}_0$ is the $M$-dimensional identity matrix, $\bar{\boldsymbol{\Lambda}}$ is the $(M^2-1)$-dimensional vector of generalized Pauli matrices [28], [33], $A_0 = |\boldsymbol{a}|^2$, and the vector $\bar{A} = \boldsymbol{a}^*\bar{\boldsymbol{\Lambda}}\boldsymbol{a}$ is the generalized Stokes vector associated to $\boldsymbol{a}$ [28]. Analogously:

$$\boldsymbol{K} = \kappa_0\boldsymbol{\Lambda}_0 + \bar{\kappa}\cdot\bar{\boldsymbol{\Lambda}}\,, \tag{27}$$

where $\kappa_0 = \beta_0 - j\alpha_0$, $\beta_0$ is the scalar phase delay per unit length, $\alpha_0$ is the scalar attenuation coefficient, and

$$\bar{\kappa} = \frac{1}{M}(\bar{\beta} - j\bar{\alpha})\,, \tag{28}$$

where $\bar{\beta}$ and $\bar{\alpha}$ are the $M$-dimensional generalized birefringence and local dichroism vectors, respectively [28]. Using these decompositions it can be proved that

$$\xi = \beta_0 + \frac{\bar{\beta}\cdot\bar{A}}{MA_0}\,, \tag{29}$$

where the first term accounts for the dynamic scalar phase $\sigma$ and the second one accounts for the dynamic mode-dependent phase $\chi$, similarly to (13) and (14), respectively.

Owing to the applied transformation, the vector $\boldsymbol{b}(z)$ is parallel transported [29], [32]; therefore, the phase $\gamma(z)$ of $\boldsymbol{b}(z)$ with respect to a reference $\boldsymbol{a}_0$ is a purely geometric phase, and can be considered a generalized Pancharatnam's phase [?], [34]. Following the guidelines of Section II-A, we consider the $z$ derivative of phase $\gamma(z)$ of $p(z) = \boldsymbol{a}_0^*\boldsymbol{b}(z)$, which is given by (10) and can be rearranged as (see Appendix B-A)

$$\partial\gamma = -\frac{\operatorname{tr}(\boldsymbol{\mathcal{A}}\boldsymbol{H}^*\boldsymbol{\mathcal{A}}_0) + \operatorname{tr}(\boldsymbol{\mathcal{A}}_0\boldsymbol{H}\boldsymbol{\mathcal{A}})}{2\operatorname{tr}(\boldsymbol{\mathcal{A}}\boldsymbol{\mathcal{A}}_0)}\,, \tag{30}$$

where $\boldsymbol{\mathcal{A}}_0$ is the coherence matrix associated to $\boldsymbol{a}_0$, $\boldsymbol{H}$ is as before defined as $\boldsymbol{H} = \boldsymbol{K} - \xi\boldsymbol{\Lambda}_0$ and we used the fact that $\boldsymbol{\mathcal{A}} = \boldsymbol{a}\boldsymbol{a}^* = \boldsymbol{b}\boldsymbol{b}^*$. The generalized Stokes vectors do not have most of the properties of the standard Stokes vectors (note for example that $A_0$ is not the modulus of $\bar{A}$) [28]; as a consequence, it is not possible to reduce (30) to a simpler expression similar to (11).

While the above considerations make explicit reference to optical fibers, they can in principle be applied also to any beam made of a superposition of propagating modes [35], provided that the optical components traversed by the beam are properly described in terms of their mode-coupling matrices.

## V. Conclusion

In this article we have analyzed the phase of a field transmitted across an optical fiber, highlighting how this phase can be decomposed into a scalar term and a polarization-dependent term, which is made itself of two contributions. The first one is the well known Pancharatnam's phase, which is geometric in nature; it depends explicitly only on the trajectory that the SOP draws on the Poincaré sphere, as given in (16). The second term is a dynamic phase depending on both the SOP and the birefringence of the fiber, according (14).

All these phase terms are implicitly taken into account by any model or experimental analysis based on the formalism of Jones matrices. Nevertheless, we believe that highlighting them can contribute to a better understanding of coherent and polarimetric optical systems. For example, in a coherent transmission system we should expect that random fluctuations of polarization contribute to phase noise. Another possible use of these results is in the framework of fiber sensing, specifically regarding the interferometric sensors and the polarimetric ones. To the best of our knowledge, almost always the former neglect polarization and the latter neglect phase; this despite the fact that interferometers have to cope with polarization and often polarimeters are based on coherent receivers. It seems reasonable to foresee that the phase decomposition analyzed here might be used to improve their accuracy.

The analysis reported in this article is mainly focused on singlemode fibers and on polarization variation as a function of either distance of propagation or frequency. Nevertheless, the theoretical framework has a much wider validity and can be applied to different scenarios. Here, we extended the analysis to multimode and multi-core fibers, showing that, while lacking an easy geometrical interpretation, the decomposition of the phase in a scalar term and a mode-dependent one is still possible.

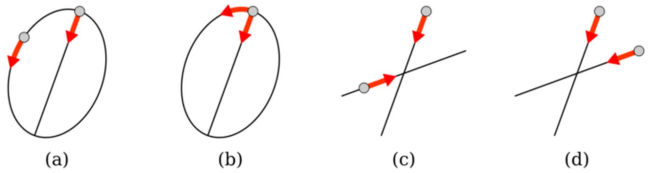


Fig. 6. Sketch of the trajectories tracked by the electric field for some polarization states. The gray dots indicate the field position at a given time $t_0$; the red arrows suggest the direction of motion as time flows.

## Appendix A
## Pancharatnam's Connection

Consider Fig. 6; comparing graphs (a) and (b) it is reasonable to state that the fields in (a) are out of phase, whereas those in (b) are in phase. Similarly, the fields in (c) are out of phase, while those in (d) are in phase. Pancharatnam's connection $\boldsymbol{a}_1^*\boldsymbol{a}_2$ captures this concept; actually, any wave $\boldsymbol{a}_2$ can be decomposed in a wave parallel to $\boldsymbol{a}_1$ and a wave orthogonal to it. Clearly, the latter one does not contribute to $\arg(\boldsymbol{a}_1^*\boldsymbol{a}_2)$, so Pancharatnam connection measures the phase difference between the component of $\boldsymbol{a}_2$ projected on $\boldsymbol{a}_1$ and $\boldsymbol{a}_1$ itself, reducing the problem of assessing the phase difference between vector waves back to a problem of phase difference between scalar (co-polarized) waves, for which we know a familiar answer. A consequence of the above observation is that as long as the wave $\boldsymbol{a}_2$ is changed only in the component orthogonal to $\boldsymbol{a}_1$, the phase difference between the two waves does not change. As an example, consider Fig. 6(b); if we change the ellipticity of the elliptical polarization by changing the length of the axis orthogonal to the linear polarization, the phase difference between the two waves does not change. On the Poincaré sphere, changing the ellipticity corresponds to moving along a meridian, which happens to be a great circle of the sphere. This result has in fact a general validity: *Pancharatnam's connection is invariant with respect to*

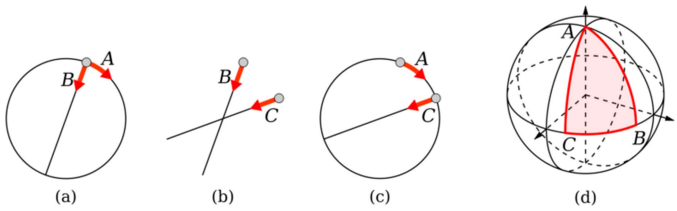


Fig. 7. Example of the non-transitivity of Pancharatnam phase.

*changes of the polarization state that occur along great circles (geodesics) of the Poincaré sphere* [29].

Pancharatnam's connection is not transitive. Regarding scalar or co-polarized waves it is evident that if a wave $A$ is in phase with a wave $B$, and $B$ is in phase with $C$, then $A$ is in phase with $C$; hence the transitivity. This does not happen for vector waves, and a simple counter example is given in Fig. 7(a)–(c): waves $A$ and $B$ are in phase, and so are $B$ and $C$; yet, waves $A$ and $C$ are clearly out of phase. It is interesting to follow the variations among the states of polarization just considered on the Poincaré sphere (Fig. 7(d)). We can move from $A$ to $B$ by collapsing the circle along the axis orthogonal to $B$; this corresponds to moving along the meridian passing through points $A$ and $B$ on the sphere; as we have seen, this does not induce variation of the phase. Moving from $B$ to $C$ corresponds to moving along the equator of the sphere; again a great circle; again no phase change. Finally, from $C$ we go back to $A$ along another meridian, again without phase variation. Nevertheless, as shown in Fig. 7(c), at the end of the process the waves are out of phase. It has been proved that this phase shift is equal to $-\Omega/2$, where $\Omega$ is the area encircled by the trajectory (or, equivalently, the solid angle subtended by that area). This result has been generalized to arbitrary open trajectories, provided that they are closed by a geodesic [29]. In conclusion, *when the polarization goes through a series of transformations, at the end of the process the wave has accrued a phase delay equal to $-\Omega/2$, where $\Omega$ is the area encircled by the trajectory that the transformations draw on the Poincaré sphere, closed by the geodesic connecting the end points of the trajectory*. This phase is purely geometric and it is called *Pancharatnam's phase*.

## Appendix B
## Mathematical Proofs

### A. Derivation of (11) and (30)

According to the transformation given by (6) and (7), the complex vector $\boldsymbol{b}(z)$ obeys (9) and hence the condition

$$\mathsf{Im}\left[\tilde{\boldsymbol{b}}^*\,\partial\tilde{\boldsymbol{b}}\right] = \mathsf{Im}\left[-j\left(\boldsymbol{a}^*\boldsymbol{Q}\boldsymbol{a} - \mathsf{Re}\left[\boldsymbol{a}^*\boldsymbol{Q}\boldsymbol{a}\right]\right)\right] = 0\,. \tag{31}$$

As remarked in Refs. [29], [32], this condition is a *parallel transport law*, in the sense that $\boldsymbol{b}(z)$ does not accumulate a dynamical phase; this leads to conclude that $\xi$ defined in (7) represents the dynamical phase delay per unit length. Recalling that $p(z) = \boldsymbol{a}_0^*\boldsymbol{b}(z)$ and $e^{j\gamma} = p/|p|$, and using (9) and (10), we have

$$p\,\partial p^* - p^*\partial p = j\boldsymbol{a}_0^*(\boldsymbol{H}\boldsymbol{\mathcal{A}} + \boldsymbol{C}\boldsymbol{\mathcal{A}}^*)\boldsymbol{a}_0 \tag{32}$$

$$= j\,\mathrm{tr}(\boldsymbol{\mathcal{A}}\boldsymbol{H}^*\boldsymbol{\mathcal{A}}_0) + j\,\mathrm{tr}(\boldsymbol{\mathcal{A}}_0\boldsymbol{H}\boldsymbol{\mathcal{A}})\,, \tag{33}$$

where $\boldsymbol{\mathcal{A}}(z) = \boldsymbol{b}(z)\boldsymbol{b}^*(z) = \boldsymbol{a}(z)\boldsymbol{a}^*(z)$ is the coherence matrix associated to $\boldsymbol{a}(z)$, $\boldsymbol{b}(z)$, and $\boldsymbol{\mathcal{A}}_0$ that associated to $\boldsymbol{a}_0$, and we used the properties of the trace $\mathrm{tr}(\cdot)$ of matrices. Exploiting the decomposition (3) for the 2-dimensional case, we can write

$$\boldsymbol{\mathcal{A}}(z) = \frac{1}{2}P(z)\left(\boldsymbol{\Lambda}_0 + \hat{s}(z)\cdot\bar{\boldsymbol{\Lambda}}\right), \tag{34}$$

with $P(z) = |\boldsymbol{a}(z)|^2$ and $\hat{s}(z)$ the unit Stokes vector associated to $\boldsymbol{a}(z)$. Let us set for brevity $\boldsymbol{H} = h_0\boldsymbol{\Lambda}_0 + \bar{\kappa}\cdot\bar{\boldsymbol{\Lambda}}$, with $h_0 = \kappa_0 - \gamma$; neglecting the factor $P/2$ we have:

$$\boldsymbol{H}\boldsymbol{\mathcal{A}} \propto (h_0\boldsymbol{\Lambda}_0 + \bar{\kappa}\cdot\bar{\boldsymbol{\Lambda}})(\boldsymbol{\Lambda}_0 + \hat{s}\cdot\bar{\boldsymbol{\Lambda}})$$

$$= (h_0 + \bar{\kappa}\cdot\hat{s})\boldsymbol{\Lambda}_0 + (h_0\hat{s} + \bar{\kappa} + j\,\bar{\kappa}\times\hat{s})\cdot\bar{\boldsymbol{\Lambda}}\,, \tag{35}$$

where we used the property of 2-dimensional Pauli matrices [36]. Since $\boldsymbol{\mathcal{A}}\boldsymbol{H}^* = (\boldsymbol{H}\boldsymbol{\mathcal{A}})^*$ we readily find

$$\boldsymbol{H}\boldsymbol{\mathcal{A}} + \boldsymbol{\mathcal{A}}\boldsymbol{H}^* \propto 2\mathsf{Re}\left[h_0 + \bar{\kappa}\cdot\hat{s}\right]\boldsymbol{\Lambda}_0$$

$$+ 2\mathsf{Re}\left[h_0\hat{s} + \bar{\kappa}\right]\cdot\bar{\boldsymbol{\Lambda}} - 2(\mathsf{Im}\left[\bar{\kappa}\right]\times\hat{s})\cdot\bar{\boldsymbol{\Lambda}}\,, \tag{36}$$

and hence

$$p\,\partial p^* - p^*\partial p = jP\left\{\mathsf{Re}\left[h_0 + \bar{\kappa}\cdot\hat{s}\right]\right.$$

$$\left. + \mathsf{Re}\left[h_0\hat{s} + \bar{\kappa}\right]\cdot\hat{s}_0 - (\mathsf{Im}\left[\bar{\kappa}\right]\times\hat{s})\cdot\hat{s}_0\right\}, \tag{37}$$

where $\hat{s}_0$ is the SOP associated to $\boldsymbol{a}_0$ and we assumed without loss of generality that $|\boldsymbol{a}_0| = 1$. Now notice that $h_0 = \kappa_0 - \xi = -j\alpha_0 - (\bar{\beta}\cdot\hat{s})/2$; therefore,

$$\mathsf{Re}\left[h_0 + \bar{\kappa}\cdot\hat{s}\right] = \mathsf{Re}\left[-j\alpha_0 - j\frac{1}{2}\bar{\alpha}\cdot\hat{s}\right] = 0\,, \tag{38}$$

$$\mathsf{Re}\left[h_0\hat{s} + \bar{\kappa}\right] = -\frac{1}{2}(\bar{\beta}\cdot\hat{s})\hat{s} + \frac{1}{2}\bar{\beta}\,. \tag{39}$$

Moreover

$$|p|^2 = \boldsymbol{a}_0^*\boldsymbol{\mathcal{A}}\boldsymbol{a}_0 = \mathrm{tr}(\boldsymbol{\mathcal{A}}\boldsymbol{\mathcal{A}}_0) = \frac{P}{2}(1 + \hat{s}\cdot\hat{s}_0)\,, \tag{40}$$

so putting everything back together we reach (30) and find:

$$\partial\gamma = \frac{[(\bar{\beta}\cdot\hat{s})\hat{s} - \bar{\beta} - \bar{\alpha}\times\hat{s}]\cdot\hat{s}_0}{2(1 + \hat{s}\cdot\hat{s}_0)} = \tag{41}$$

$$= -\frac{[(\bar{\beta}\times\hat{s}) - \bar{\alpha}]\cdot(\hat{s}_0\times\hat{s})}{2(1 + \hat{s}\cdot\hat{s}_0)}\,. \tag{42}$$

Finally, recalling that[1]

$$\partial\hat{s} = \bar{\beta}\times\hat{s} + \hat{s}\times\hat{s}\times\bar{\alpha}\,, \tag{43}$$

we reach (11).

### B. Geometrical Interpretation of (11) and (16)

We now prove that when integrated along the fiber length, i.e. from $z = 0$ to $L$, (11) yields a value equal to $-1/2$ times the area on the Poincaré sphere encircled by the trajectory that goes from $\hat{s}_0$ to $\hat{s}(0)$ along the geodesic, then follows $\hat{s}(z)$ and finally goes back to $\hat{s}_0$ along the geodesic that connects $\hat{s}(L)$ to $\hat{s}_0$ (see Fig. 8). Note that, the "area" should be taken positive if the trajectory is "right handed", i.e. consistent with a counterclockwise rotation around $\hat{s}_0$.

Consider the generic infinitesimal area, $d\Omega$, delimited by the geodesic from $\hat{s}_0$ to $\hat{s}(z)$, the section of SOP trajectory going

[1]The plus sign in this equation stems from the definition $\bar{\kappa} = (\bar{\beta} - \bar{\alpha})/2$ introduced in (5). Note that some authors define $\bar{\alpha}$ with the opposite sign.

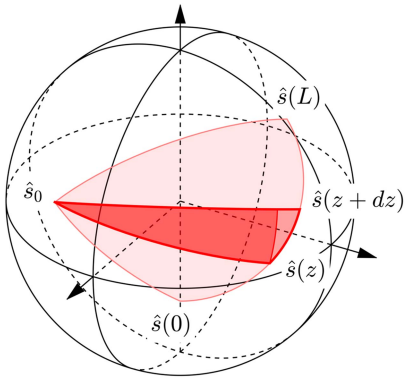


Fig. 8. Representation of the infinitesimal surface spanned by an infinitesimal variation of the SOP.

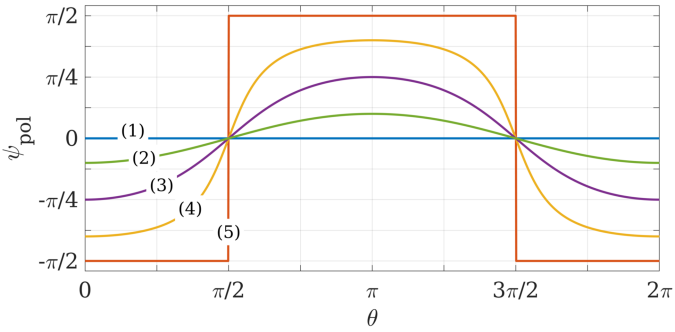


Fig. 9. Polarization-dependent phase accumulated by a light beam as it traverse a birefringence waveplate with different thicknesses: (1) $L = L_B$, full waveplate; (2) $L = L_B/10$; (3) $L = L_B/4$, quarter waveplate; (4) $L = 2L_B/5$; (5) $L = L_B/2$, half waveplate.

from $\hat{s}(z)$ to $\hat{s}(z+dz)$, and the geodesic from $\hat{s}(z+dz)$ to $\hat{s}_0$ (Fig. 8). This area can be decomposed in two parts: the first one, $d\Omega_1$ (darker in the figure), is obtained by rotating $\hat{s}(z)$ around $\hat{s}_0$ until the geodesic passing through $\hat{s}_0$ and $\hat{s}(z+dz)$ is meet; the second part, $d\Omega_2$, is simply the rest. Since $d\Omega_1$ is obtained by a rotation around $\hat{s}_0$, it is actually a wedge of a spherical cap and its area is

$$d\Omega_1 = \mu_0(1-\cos\theta) = \mu_0\big(1-\hat{s}_0\cdot\hat{s}(z)\big)\,, \tag{44}$$

where $\mu_0$ is the angle at the vertex $\hat{s}_0$ and $\theta$ is the angle subtended by $\hat{s}_0$ and $\hat{s}(z)$. The angle $\mu_0$ is the angle subtended by the plane defined by $\hat{s}_0$ and $\hat{s}(z)$ and the plane defined by $\hat{s}_0$ and $\hat{s}(z+dz)$; therefore, it is also the angle subtended by the normals to those planes. Mathematically, we have

$$|\sin\mu_0| = \frac{\big|(\hat{s}_0\times\hat{s})\times\big(\hat{s}_0\times(\hat{s}+d\hat{s})\big)\big|}{|\hat{s}_0\times\hat{s}|\,|\hat{s}_0\times(\hat{s}+d\hat{s})|} \approx \frac{|d\hat{s}\cdot(\hat{s}_0\times\hat{s})|}{|\hat{s}_0\times\hat{s}|^2}\,, \tag{45}$$

where we set $\hat{s}(z+dz)\approx\hat{s}+d\hat{s}$. Considering that $\mu_0$ is infinitesimal and that it is positive if $d\hat{s}$ "makes the plane $\{\hat{s}_0,\,\hat{s}\}$ rotate" counterclockwise around $\hat{s}_0$, we can write

$$\mu_0 \approx \frac{d\hat{s}\cdot(\hat{s}_0\times\hat{s})}{|\hat{s}_0\times\hat{s}|^2} = \frac{d\hat{s}\cdot(\hat{s}_0\times\hat{s})}{1-(\hat{s}_0\cdot\hat{s})^2}\,. \tag{46}$$

Combining this with (44) we get

$$d\Omega_1 \approx \frac{d\hat{s}\cdot(\hat{s}_0\times\hat{s})}{1+\hat{s}_0\cdot\hat{s}}\,. \tag{47}$$

Regarding the second part of the area, note that as $dz$ tends to 0, the area collapses in a point, approximating a flat triangle. More specifically, all the sides of this triangle are proportional to $|d\hat{s}|$, therefore the area $d\Omega_2$ is an infinitesimal of order 2, whereas $d\Omega_1$ is infinitesimal of order 1. As a consequence, $d\Omega_2$ plays no role in the Riemann sum that leads to the integration, proving the starting hypothesis.

## Appendix C
## PDP in simple waveplates

We analyze here for completeness the PDP in simple optical waveguides as birefringent waveplates and ideal polarizers.

### A. *Birefringent Waveplate*

An interesting case of study is that of a birefringent waveplate with $\bar{\beta}$ constant and $\bar{\alpha}=0$; this is the typical elementary building block in the numerical representation of birefringent fibers [27]. We are interested in studying how the phase of the output wave changes with respect to the input one; so we set $\boldsymbol{a}_0 = \boldsymbol{a}(0)$ — and hence $\hat{s}_0 = \hat{s}(0)$. Then, the transmitted SOP can be expressed as [27]

$$\hat{s}(z) = \hat{s}_0 + (\sin\beta z)(\hat{\beta}\times\hat{s}_0) + (1-\cos\beta z)(\hat{\beta}\times\hat{\beta}\times\hat{s}_0)\,, \tag{48}$$

where $\beta = |\bar{\beta}|$, and $\hat{\beta} = \bar{\beta}/\beta$. The dynamic polarization-dependent phase reads simply

$$\chi(z) = -\frac{1}{2}(\beta\cos\theta)z \tag{49}$$

where $\theta$ is the (constant) angle subtended by $\bar{\beta}$ and $\hat{s}_0$. Regarding the geometric term, using (48) and (16), and recalling that $\partial\hat{s} = \bar{\beta}\times\hat{s}$, we find

$$\partial\gamma = -\frac{\beta}{2}\,\frac{(1-\cos\beta z)\sin^2\theta\,\cos\theta}{2-(1-\cos\beta z)\sin^2\theta}\,. \tag{50}$$

Integrating this expression and summing the result to $\chi(z)$ we finally reach the expression of the PDP of a waveplate:

$$\psi_{\text{pol}} = -\arctan\left(\cos\theta\cdot\tan\left(\pi L/L_B\right)\right), \tag{51}$$

where $L$ is the length of the waveplate and $L_B = 2\pi/\beta$ is its beat length. Fig. 9 shows $\psi_{\text{pol}}$ as a function of $\theta$, for different lengths $L$; there are some interesting features to comment. The so called full-wave plate (FWP, curve (1) in the figure) has thickness equal to an integer multiple of $L_B$, hence it does not vary the polarization; we see here that it doesn't vary the PDP neither. Nevertheless, the FWP has a non-zero geometric phase, which is however exactly compensated by the dynamic polarization-dependent term [37]. The half-wave plate (HWP, curve (5)) induces a $\theta$-independent phase shift, which however abruptly changes sign as soon as the sign of $\cos\theta$ changes. Differently, the PDP of a quarter-wave plate (QWP, curve (3)) varies smoothly with $\theta$. The extreme values of $\psi_{\text{pol}}$ are obtained for either $\theta = 0$ or $\theta = \pi$, which correspond to the input SOP being aligned with one of the two optical axes of the waveplate—i.e. the conditions in which the input SOP is not changed.

### B. Polarizer

A polarizer can be modelled as a device with constant dichroism axes and negligible birefringence, which correspond to setting $\bar{\alpha}$ constant with respect to $z$ and $\bar{\beta} = 0$. In this case, the propagation across the waveplate corresponds to moving the SOP on the Poincaré sphere along the great circle passing through $\bar{\alpha}$ and the input SOP, $\hat{s}_0$; hence the propagation across an ideal polarizer does not induce Pancharatnam's phase.

To prove this, notice that if $\hat{s}$ moves along the great circle passing through $\hat{s}_0$ and $\bar{\alpha}$, then $\hat{s}$ must be always orthogonal to $\hat{s}_0 \times \bar{\alpha}$. Using (43) with $\bar{\beta} = 0$, it is straightforward to show that

$$\partial\big[(\hat{s}_0 \times \bar{\alpha}) \cdot \hat{s}\big] = (\bar{\alpha} \cdot \hat{s})\big[(\hat{s}_0 \times \bar{\alpha}) \cdot \hat{s}\big]\,; \tag{52}$$

for $z = 0$ we have $\hat{s}(0) = \hat{s}_0$ and $(\hat{s}_0 \times \bar{\alpha}) \cdot \hat{s}(0) = 0$, hence $\partial\big[(\hat{s}_0 \times \bar{\alpha}) \cdot \hat{s}(z = 0)\big] = 0$, proving that $(\hat{s}_0 \times \bar{\alpha}) \cdot \hat{s}(z) = 0$ is the solution of (52), and thus that the trajectory is the said great circle. Further calculation would show that the SOP tends to be parallel to $-\bar{\alpha}$, which is the SOP with least attenuation.

Incidentally, notice also that this result is (of course) consistent with the fact that moving along a geodesic does not change the Pancharatnam's phase. Indeed, for $\bar{\beta} = 0$ and using again (43), (11) yields

$$\partial\gamma = \frac{(\hat{s}_0 \times \bar{\alpha}) \cdot \hat{s}}{1 + \hat{s} \cdot \hat{s}_0}\,, \tag{53}$$

which is 0 if $\bar{\alpha}$ is constant, as proved above.

## References


[1] S. Pancharatnam, "Generalized theory of interference, and its applications," *Proc. Indian Acad. Sci. - Sect. A*, vol. 44, pp. 247–262, 1956.

[2] M. V. Berry, "Quantal phase factors accompanying adiabatic changes," *Proc. Roy. Soc. London. Ser. A., Math. Phys. Sci.*, vol. 392, no. 1802, pp. 45–57, 1984.

[3] S. Ramaseshan and R. Nityananda, "The interference of polarized light as an early example of berry's phase," *Curr. Sci.*, vol. 55, no. 24, pp. 1225–1226, Dec. 1986.

[4] M. V. Berry, "The adiabatic phase and pancharatnam's phase for polarized light," *J. Modern Opt.*, vol. 34, no. 11, pp. 1401–1407, 1987.

[5] E. Cohen, H. Larocque, F. Bouchard, F. Nejadsattari, Y. Gefen, and E. Karimi, "Geometric phase from aharonov to pancharatnam and beyond," *Nature Rev. Phys.*, vol. 1, no. 7, pp. 437–449, Jul. 2019.

[6] Z. Ma and S. Ramachandran, "Propagation stability in optical fibers: Role of path memory and angular momentum," *Nanophotonics*, vol. 10, no. 1, pp. 209–224, Jan. 2021.

[7] C. P. Jisha, S. Nolte, and A. Alberucci, "Geometric phase in optics: From wavefront manipulation to waveguiding," *Laser Photon. Rev.*, vol. 15, no. 10, 2021, Art. no. 2100003.

[8] N. R. Sadykov, "Rytov-vladimirsky polarization effect," *Opt. Spectrosc.*, vol. 92, no. 4, pp. 584–587, Apr. 2002.

[9] R. Y. Chiao and Y.-S. Wu, "Manifestations of berry's topological phase for the photon," *Phys. Rev. Lett.*, vol. 57, no. 8, pp. 933–936, 1986.

[10] A. Tomita and R. Y. Chiao, "Observation of berry's topological phase by use of an optical fiber," *Phys. Rev. Lett.*, vol. 57, no. 8, pp. 937–940, 1986.

[11] M. V. Berry, "Interpreting the anholonomy of coiled light," *Nature*, vol. 326, no. 6110, pp. 277–278, 1987.

[12] J. N. Ross, "The rotation of the polarization in low birefringence monomode optical fibres due to geometric effects," *Opt. Quantum Electron.*, vol. 16, no. 5, pp. 455–461, Sep. 1984.

[13] F. D. M. Haldane, "Path dependence of the geometric rotation of polarization in optical fibers," *Opt. Lett.*, vol. 11, no. 11, pp. 730–732, Nov. 1986.

[14] K. Itoh, T. Saitoh, and Y. Ohtsuka, "Optical rotation sensing by the geometric effect of fiber-loop twisting," *J. Lightw. Technol.*, vol. 5, no. 7, pp. 916–919, Jul. 1987.

[15] J. Segert, "Photon berry's phase as a classical topological effect," *Phys. Rev. A*, vol. 36, no. 1, pp. 10–15, Jul. 1987.

[16] E. M. Frins and W. Dultz, "Direct observation of berry's topological phase by using an optical fiber ring interferometer," *Opt. Commun.*, vol. 136, no. 5, pp. 354–356, Apr. 1997.

[17] E. I. Yakubovich and G. B. Malykin, "The effect of noncoplanar winding of an optical fiber in a fiber ring interferometer on the phase difference of counterpropagating waves," *Radiophysics Quantum Electron.*, vol. 45, no. 11, pp. 895–905, 2002.

[18] L. Palmieri, "Accurate distributed characterization of polarization properties in optical fibers," in *Proc. IEEE 36th Eur. Conf. Opt. Commun.*, 2010, pp. 1–6.

[19] L. Palmieri, "Distributed polarimetric measurements for optical fiber sensing," *Opt. Fiber Technol.*, vol. 19, no. 6, Part B, pp. 720–728, 2013.

[20] E. Bortolotti, "Sulle rappresentazioni conformi, e su di una interpretazione fisica del parallelismo di Levi-Civita," *Atti Della Reale Accademia Nazionale Dei Lincei*, vol. IV, pp. 552–556, 1926.

[21] M. Martinelli and P. Vavassori, "A geometric (Pancharatnam) phase approach to the polarization and phase control in the coherent optics circuits," *Opt. Commun.*, vol. 80, no. 2, pp. 166–176, Dec. 1990.

[22] C. N. Alexeyev and M. A. Yavorsky, "Topological phases in a weakly guiding elliptic twisted fiber," in *Proc. IEEE CAOL 1st Int. Conf.*, 2003, pp. 62–65.

[23] J. Ferrari, E. Frins, and W. Dultz, "Optical fiber vibration sensor using (Pancharatnam) phase step interferometry," *J. Lightw. Technol.*, vol. 15, no. 6, pp. 968–971, Jun. 1997.

[24] G. B. Malykin and V. I. Pozdnyakova, "Geometric phases in singlemode fiber lightguides and fiber ring interferometers," *Phys.-Uspekhi*, vol. 47, no. 3, pp. 289–308, Mar. 2004.

[25] S. Shaheen and K. Hicke, "Geometric phase in distributed fiber optic sensing," *Opt. Lett.*, vol. 47, no. 15, Aug. 2022, Art. no. 3932.

[26] S. Ramaseshan, "The poincare sphere and the pancharatnam phase - some historical remarks," *Curr. Sci.*, vol. 59, no. 21\22, pp. 1154–1158, Nov. 1990.

[27] J. P. Gordon and H. Kogelnik, "PMD fundamentals: Polarization mode dispersion in optical fibers," *Proc. Nat. Acad. Sci.*, vol. 97, pp. 4541–4550, 2000.

[28] C. Antonelli, A. Mecozzi, M. Shtaif, and P. J. Winzer, "Stokes-space analysis of modal dispersion in fibers with multiple mode transmission," *Opt. Exp.*, vol. 20, no. 11, pp. 11718–11733, 2012.

[29] J. Samuel and R. Bhandari, "General setting for berry's phase," *Phys. Rev. Lett.*, vol. 60, no. 23, pp. 2339–2342, Jun. 1988.

[30] M. Reimer and D. Yevick, "Least-squares analysis of the mueller matrix," *Opt. Lett.*, vol. 31, no. 16, pp. 2399–2401, Aug. 2006.

[31] H. Lefevre, "Single-mode fibre fractional wave devices and polarisation controllers," *Electron. Lett.*, vol. 16, no. 20, pp. 778–780, Sep. 1980.

[32] Y. Aharonov and J. Anandan, "Phase change during a cyclic quantum evolution," *Phys. Rev. Lett.*, vol. 58, no. 16, pp. 1593–1596, Apr. 1987.

[33] M. Gell-Mann, "Symmetries of baryons and mesons," *Phys. Rev.*, vol. 125, no. 3, pp. 1067–1084, Feb. 1962.

[34] G. Milione, S. Evans, D. A. Nolan, and R. R. Alfano, "Higher order pancharatnam-berry phase and the angular momentum of light," *Phys. Rev. Lett.*, vol. 108, no. 19, May 2012.

[35] E. J. Galvez, P. R. Crawford, H. I. Sztul, M. J. Pysher, P. J. Haglin, and R. E. Williams, "Geometric phase associated with mode transformations of optical beams bearing orbital angular momentum," *Phys. Rev. Lett.*, vol. 90, no. 20, May 2003, Art. no. 203901.

[36] A. Galtarossa and L. Palmieri, "Theoretical analysis of reflectometric measurements in optical fiber links affected by polarization-dependent loss," *J. Lightw. Technol.*, vol. 21, no. 5, pp. 1233–1241, May 2003.

[37] G. D. Love, "The unbounded nature of geometrical and dynamical phases in polarization optics," *Opt. Commun.*, vol. 131, no. 4, pp. 236–240, Nov. 1996.